

Spin Wave Optics

Kirill A. Rivkin

RKMAG Corporation, 651 N. Broad St. Suite 205 462 Middletown Delaware 19709

Similarity between Walker and Helmholtz equations encouraged many to search for analogies between optical and spin wave phenomena. In the present article we demonstrate that one to one relationship can be established by formalizing the concept of “magnetic refractive index” and deriving on its basis Eikonal equations for magnetic media, formally proving that a very substantial portion of optical devices: lenses, mirrors, waveguides and so on, can be implemented as magnetic devices operating on spin waves instead of optical radiation. Controlling the refractive index is accomplished by changing the environmental variables such as magnetic bias field or temperature. Functionality of the above mentioned devices is confirmed with micromagnetic simulations, which also demonstrate a substantial agreement with the analytical model introduced in the present manuscript.

In the last three decades there has been a considerable number of publications demonstrating spin wave lensing or other manner of spin wave control, often in relation with computing applications^{1,2}. Most common approach relies on physical alteration of the magnetic media^{3,4,5}, such as thinning out specific sections, physically shaping the waveguides or using inserts made from different materials. Some of the published ideas were inspired by optical concepts^{6,7} and the term “refractive index” has been introduced to describe behavior of magnetic systems⁸ in a context of specific, predominantly numerically studied cases. It remained unclear whether more general or analytical formula-based approach is feasible or there is a more fundamental difference between the formulations related to optical and magnetic wave propagation.

With this in mind let us begin with a general point, which is a propagation of spin waves in magnetic media subject to varied environmental variables, for example, the bias field or temperature; in the latter case we assume that impact is due to temperature dependence of the saturation magnetization.

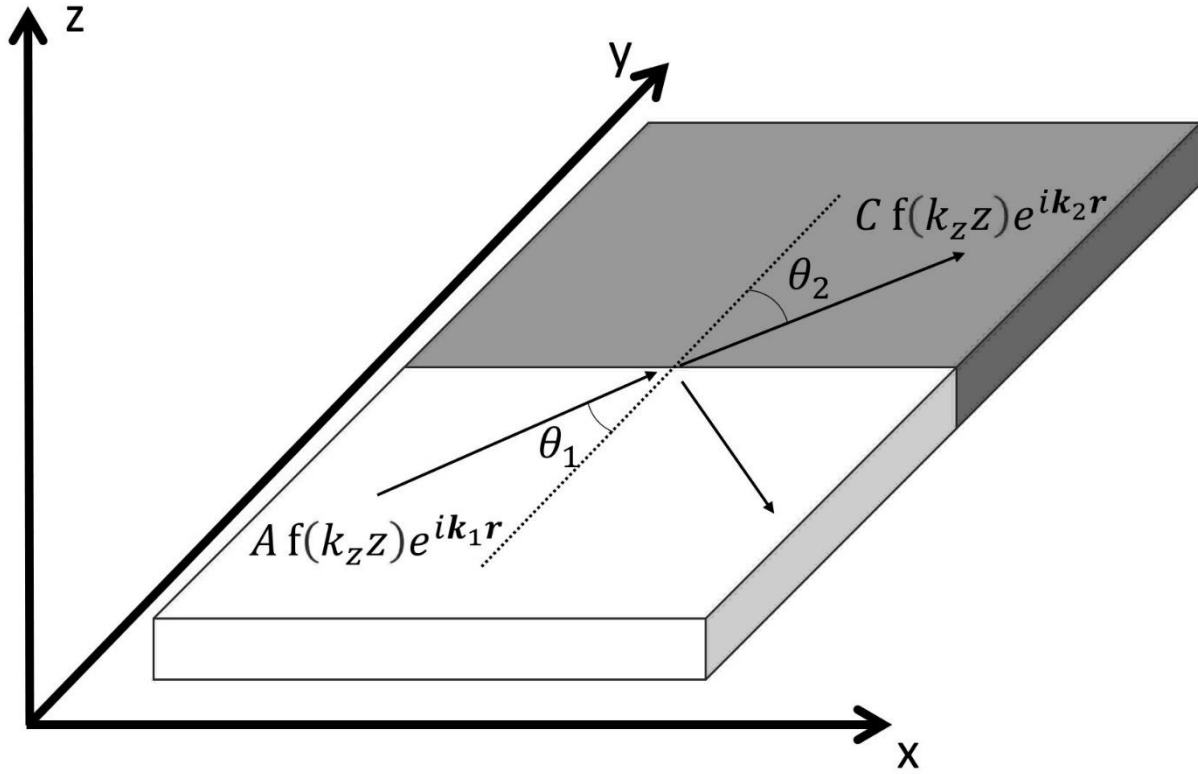


Figure 1. Schematic display illustrating a plane wave $Af(k_z z)e^{ik_1 r}$ with amplitude A and wavevector k_1 impacting at the angle θ_1 the boundary between the two segments characterized by different values of χ . Transmitted wave propagates at an angle θ_2 with a wavevector k_2 and amplitude C .

Consider the case where the media can be separated into two segments (Fig. 1) each subjected to a specific bias field or temperature. Entire sample is saturated in the out of plane direction due to the uniform external magnetic field H_0 applied along the z axis. Let there be an additional out of plane spatially dependent field component ΔH whose values are different in the two segments. The equation for magnetic potential φ has the form⁹:

$$(1 + \chi) \left[\frac{\partial^2 \varphi}{\partial x^2} + \frac{\partial^2 \varphi}{\partial y^2} \right] + \frac{\partial^2 \varphi}{\partial z^2} = 0 \quad (1)$$

$$\chi = \frac{\omega_0 \omega_M}{\omega_0^2 - \omega^2} \quad \omega_M = \gamma \mu_0 M_s \quad \omega_0 = \gamma \mu_0 (H_0 + \Delta H - M_s)$$

Where M_s is saturation magnetization, γ is gyromagnetic ratio, ω is the frequency at which spin waves are excited. To account for the exchange interaction⁹ additional component Dk^2 proportional to wavevector amplitude squared can be added to ω_0 .

Difference between the segments is denoted by different values of $\chi_{1,2}$; given plane wave solutions in both (Fig.1), tangential boundary conditions ensure that the reflection angle is equal to the incident one and the incident and transmitted wavevectors $k_{1,2}$ relate as:

$$\frac{\sin\theta_1}{\sin\theta_2} = \frac{k_2}{k_1} \quad (2).$$

By analogy with optics a refractive index of magnetic media⁸ can be defined as $\frac{k_2}{k_1} = \frac{n_2}{n_1}$.

Assuming magnetic potential's form $\varphi = \varphi(x, y) \cos(k_z z)$ we can derive the expression for n by using the equivalence (due to boundary conditions) of k_z in both segments, accordingly obtaining from (Eq. 1) the equation for $\frac{n_2}{n_1}$. For the out of plane saturated media it is:

$$n_{1,2} = \frac{i}{\sqrt{(1+\chi_{1,2})}} \quad (3).$$

The purpose of i is to match the real values of n with the allowed propagation frequencies band. Continuity of the normal flux across the boundary connects the amplitudes of reflected B , incoming A and transmitted signal $C = A + B$:

$$B = A \left(\frac{2\cos\theta_1}{in_1^2(\kappa_1 - \kappa_2)\sin\theta_1 + \cos\theta_1 + \frac{n_1}{n_2}\cos\theta_2} - 1 \right) \quad (4),$$

where $\kappa = \frac{\omega\omega_M}{\omega_0^2 - \omega^2}$. For the normal incidence (Eq.4) becomes identical to its optical counterpart known as Fresnel equation: $B = A \left(\frac{n_2 - n_1}{n_2 + n_1} \right)$.

Since in most cases magnetic refractive index is a relative metric, it is convenient to consider a "base" media with a constant refractive index n_0 and a wavevector k_0 , and characterize segments with spatially dependent refractive index n using a relative value $\hat{n} = \frac{n}{n_0}$. In this notation (Eq.1) transforms into Helmholtz-like equation for spin waves:

$$\left[\frac{\partial^2 \varphi(x,y)}{\partial x^2} + \frac{\partial^2 \varphi(x,y)}{\partial y^2} \right] + \hat{n}^2 k_0^2 \varphi(x, y) = 0 \quad (5).$$

We can obtain a general expression characterizing a spin wave path using Eikonal approach: assuming the form $\varphi = \varphi_0 e^{ik_0 \mathcal{L}(x,y)}$ and that \hat{n} varies on a much larger scale compared to k_0 . In this case¹⁷ in the second derivatives in (Eq.5) we can neglect all terms except those proportional to k_0^2 , obtaining:

$$\left(\left(\frac{\partial \mathcal{L}}{\partial x} \right)^2 + \left(\frac{\partial \mathcal{L}}{\partial y} \right)^2 \right) = \hat{n}^2 \quad (6),$$

which is identical to Eikonal equation for optics¹⁷. This means an arbitrary device or phenomena relying on geometric optics can be reproduced using spin waves by providing a geometrically similar magnetic refractive index n . It can be accomplished, for example, by using magnetic bias fields with the necessarily spatial distribution and amplitude. Noting that (Eqs.5-6) depend only on a relative and not the absolute value of refractive index it is possible to redefine the refractive index in the manner that $\hat{n} = 1$ for a chosen value of the bias field H_0 , and for an additional bias field ΔH : $\hat{n} = \frac{\sqrt{(1+\chi(H_0))}}{\sqrt{(1+\chi(H_0+\Delta H))}}$

For the in plane magnetized case the derivation is more complicated since the magnetic refractive index is anisotropic and depends on the angle φ between the wavevector \mathbf{k} and the in plane applied field's direction. (Eq.1) remains applicable, with z axis now corresponding to the inplane direction parallel to

the applied field, and y axis denoting the out of plane direction. Assuming media properties are homogeneous along the y axis gives a straightforward expression for both volume and surface waves:

$$\frac{k_1}{k_2} = \frac{-\left(\frac{\cos^2 \varphi_2}{(1+\chi_2)} + \sin^2 \varphi_2\right)}{-\left(\frac{\cos^2 \varphi_1}{(1+\chi_1)} + \sin^2 \varphi_1\right)} \quad (7).$$

However, we argue that the refractive index is best defined using Eikonal equation. Considering the case where majority of the media is characterized by a constant χ_0 and some specific angle between the wavevector and field axis φ_0 , in the limit of slow spatial variation of χ (Eq.1) becomes:

$$\frac{1}{n_{0x}^2} \left(\frac{\partial \mathcal{L}}{\partial x}\right)^2 + \frac{1}{n_{0x}^2 n_z^2} \left(\frac{\partial \mathcal{L}}{\partial z}\right)^2 = 1 \quad (8).$$

$$n_{0x}^2 = -\left(\frac{\cos^2 \varphi_0}{(1+\chi_0)} + \sin^2 \varphi_0\right) \quad n_z^2 = 1 + \chi$$

Because of intrinsic complexity related to birefringence of the media, henceforth we will consider only out of plane saturated examples, noting that similar devices have been modeled for the inplane case as well. When spin wave propagation lacks reciprocity, (Eq.5) or its analogue can be rewritten as a multiplication of positive and negative direction wave propagation equations.

Let us consider how for the out-of-plane saturated case the value of \acute{n} depends on the additional bias field ΔH (Fig. 2).

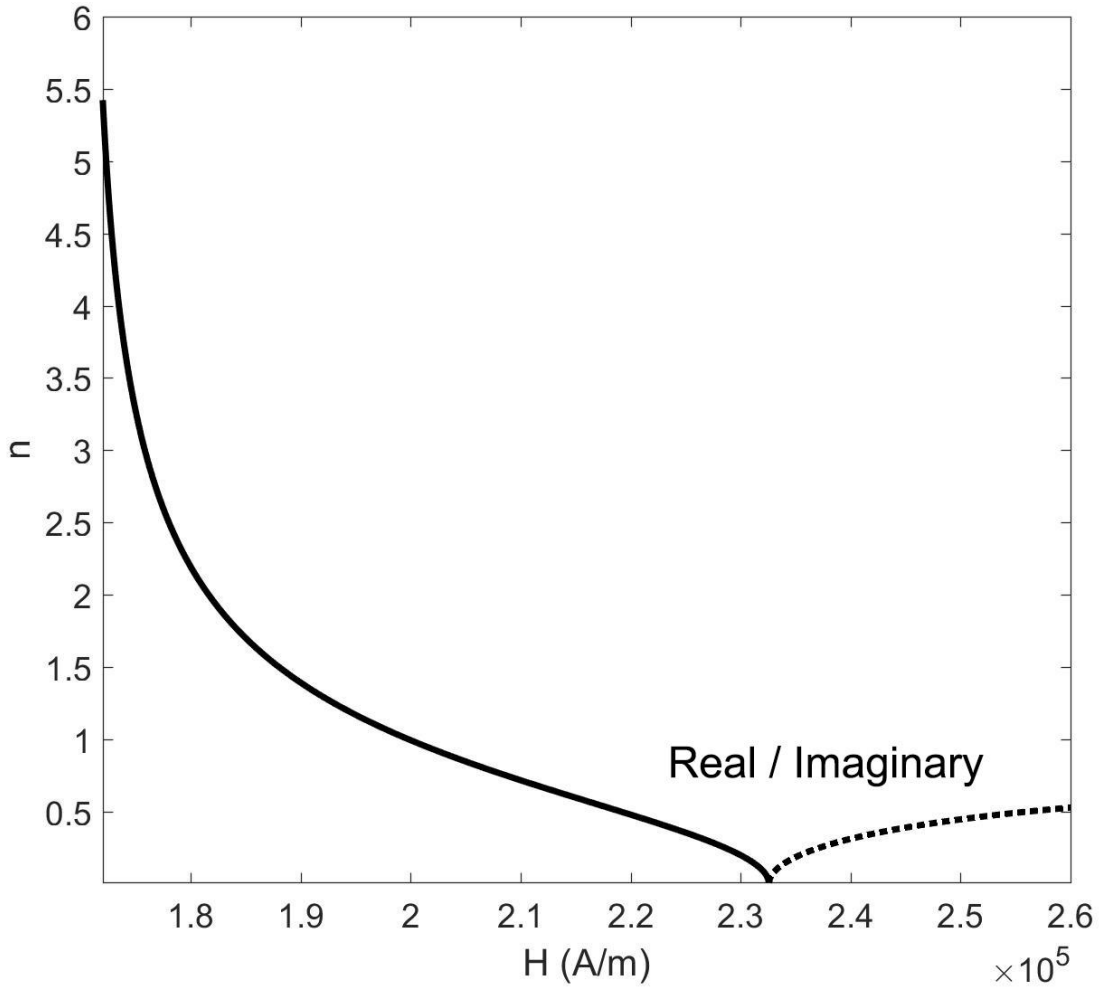


Figure 2. Magnetic refractive index as a function of the total magnetic bias field $H = H_0 + \Delta H$ for a fixed frequency $\omega = 2.4$ GHz. There is a transition from real to imaginary values occurring around $2.32 \cdot 10^5$ A/m.

In the magnetostatic approximation for any given total bias field $H_0 + \Delta H$ there is a specific range of frequencies available for excitation: if ΔH is large enough (Fig. 2) so that $\gamma\mu_0\Delta H > \omega - \omega_0$, the value of n becomes imaginary since even the uniform mode has a frequency higher than ω_0 and propagating waves cannot be excited. Instead, there is an exponentially decaying solution where the incident wave is reflected back. Noted, unlike metals in magnetostatics there are no currents being generated and thus plasmonic phenomena are absent, though boundary-localized modes typically can be excited.

For a small ΔH a relative refractive index can be approximated as:

$$\hat{n} = \frac{n(H+\Delta H)}{n(H)} \approx 1 - \frac{1}{2} \frac{\gamma\mu_0\Delta H}{\omega_0} \left(\frac{\omega^2 + \omega_0^2}{\omega^2 - \omega_0^2} \right) \quad (9),$$

noting the expression's accuracy is reduced in the vicinity of both low and high threshold values of ΔH (Fig.2). It is also applicable when n is affected by the local reduction of saturation magnetization - via temperature profile, geometry changes or otherwise: resulting decrease of the demagnetization field is effectively equivalent to the proportional increase of the bias field, i.e. $\Delta H > 0$ and the refractive index of the impacted area is decreased compared to the rest of the media. In addition, changing media thickness also impacts the boundary conditions increasing the imaginary component of the refractive index as well.

Using (Eqs. 6 and 9) we can reproduce a near arbitrary optical design by creating an identical spatial distribution of the refractive index. Resulting functionality is verified via micromagnetic modeling performed with RKMAG code¹⁵. Material parameters chosen are representative of Yttrium Garnet¹⁴ (YIG), $\mu_0 M_s = 0.18$ T, exchange stiffness $A = 3.65 \cdot 10^{-12}$ J/m, damping parameter $\beta = 0.0004$, thickness 15nm with discretization cell 15x15x15nm, i.e. below the exchange length¹⁰. Typical size of modeled sample was 35 by 35 micrometers; in order to suppress the boundary reflections, which otherwise result in a discrete resonance spectrum, we borrowed a trick from the optical FDTD models by introducing 180nm wide layer along the edges where the damping gradually increases to 1.

In general case convergence of micromagnetic and magnetostatic solutions derived from Eq.1 is not a given. Minor divergences are caused by the micromagnetic assumption that thickness dependence is uniform, which remains satisfactory for very thin films, and there is a micromagnetic cutoff in the dynamic magnetic fields due to a finite sample size being modeled. More importantly however, (Eq.1) is derived on the assumption of environmental variables changing instantaneously in space. In practical situations the variation is expected to be continuous and Maxwell's equation $-\nabla \cdot \mu \nabla \varphi = 0$ leads to:

$$(1 + \chi) \left[\frac{\partial^2 \varphi}{\partial x^2} + \frac{\partial^2 \varphi}{\partial y^2} \right] + \frac{\partial^2 \varphi}{\partial z^2} + \frac{\partial \chi}{\partial x} \frac{\partial \varphi}{\partial x} - i \frac{\partial \kappa}{\partial x} \frac{\partial \varphi}{\partial y} + i \frac{\partial \kappa}{\partial y} \frac{\partial \varphi}{\partial x} + \frac{\partial \chi}{\partial y} \frac{\partial \varphi}{\partial y} = 0 \quad (10).$$

It can be shown that in most cases the impact due to additional terms in (Eq.10) is limited to additional reflections roughly proportional to the gradient of n . In particular in geometric optics approximation the relationships in (Eqs. 2-9) remain valid.

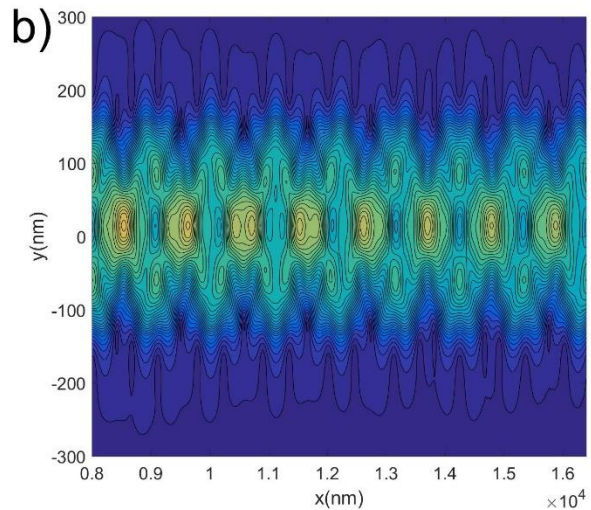
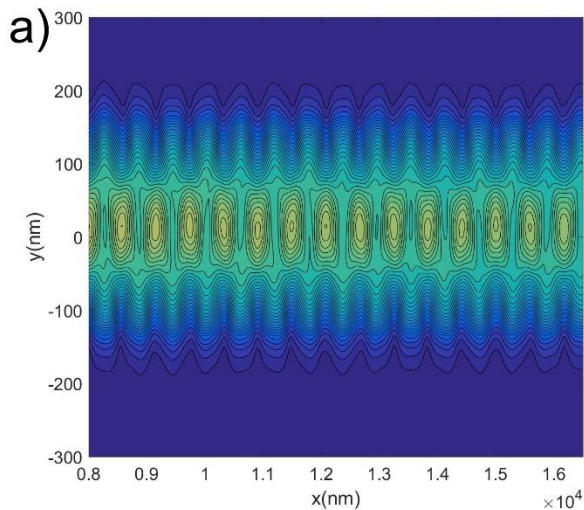


Figure 3. Micromagnetically modeled amplitude of steady state spin wave excitations for a waveguide solution where a bias field $H_0 = 2 \cdot 10^5$ A/m saturates the sample in the out of plane direction, and the additional field $\Delta H = 8 \cdot 10^4$ A/m Oe is applied everywhere except for 300 nm wide “waveguide” in the center, creating a “cladding” with an imaginary magnetic refractive index. **(a)** $\omega = 3.8$ GHz **(b)** $\omega = 11.4$ GHz.

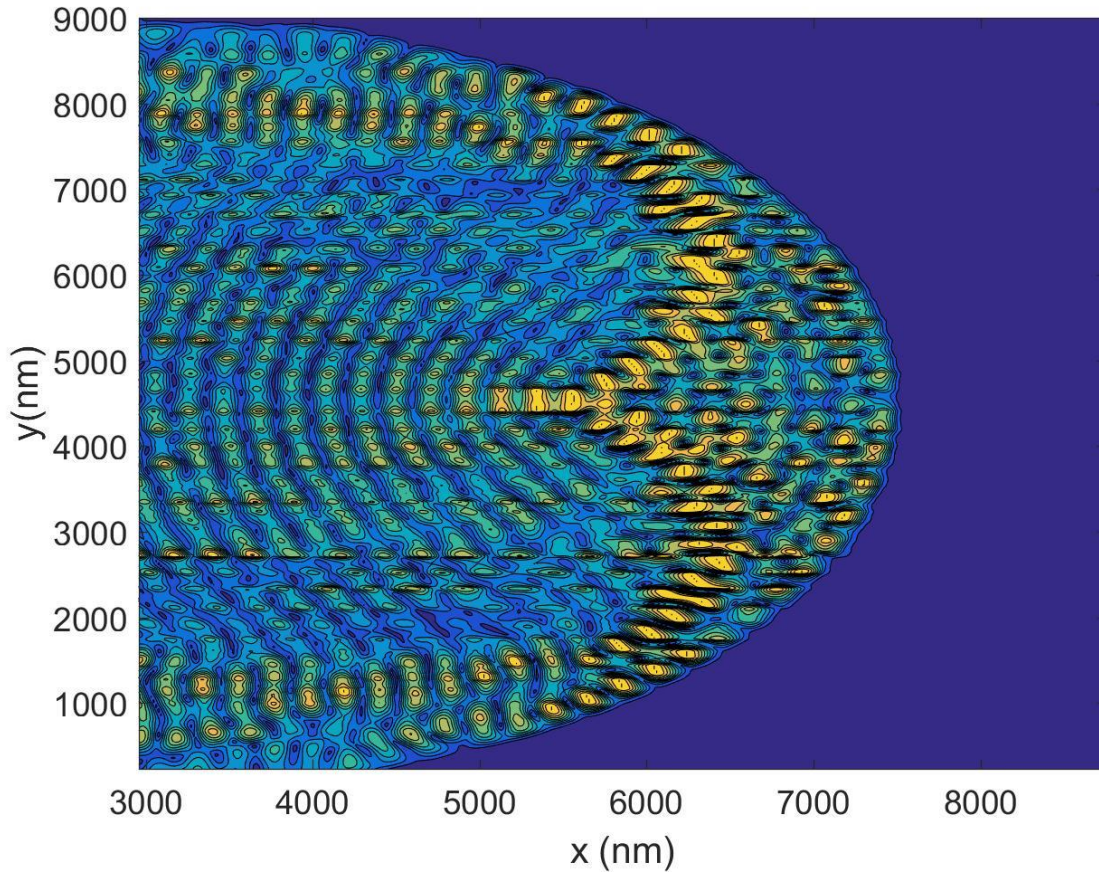


Figure 4. Modeled amplitude of spin wave excitations for a reflective lens where a bias field $H_0 = 2 \cdot 10^5$ A/m saturates the sample in the out of plane direction, and the additional field $\Delta H = 5 \cdot 10^4$ A/m is applied in a concave shape creating a focusing mirror. $\omega = 3$ GHz.

Simplest “spin optical” devices are those utilizing reflections, since once the field exceeds the threshold value (Fig. 2) there is limited sensitivity to all parameters including the dispersion of n , as evident in the modeling of a waveguide with a reflective casing (Fig. 3) and a reflective lens (Fig. 4) whose functionality has a weak dependence on the operating frequency.

Refractive devices can be modeled by solving (Eq. 5) or (Eq.6), or using an equivalent raytracing model (Figs. 5,6). Consider a typical refractive lens (Fig. 5) formed by two surfaces specified by curvature radii. Applying an additional bias field ΔH between the surfaces reproduces the raytracing solution for the corresponding (Eq. 9) relative refractive index \acute{n} , diffractive aberration notwithstanding.

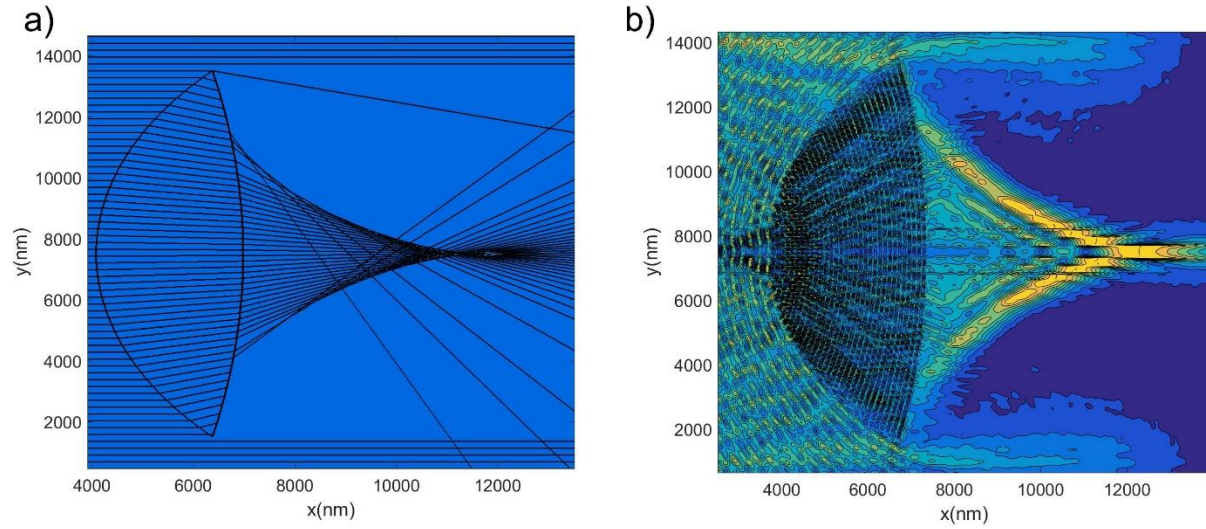


Figure 5. (a) Raytracing model for a lens bounded by the surface with respective curvature $R_2 = 30$ micrometers and $R_1 = 9$ micrometers, $n_{21} = 2.3$; **(b)** steady state magnetostatic mode amplitudes for an equivalent refractive lens formed by applying $\Delta H = -0.18 \cdot 10^5$, $\omega = 3$ GHz, $H_0 = 2 \cdot 10^5$ A/m.

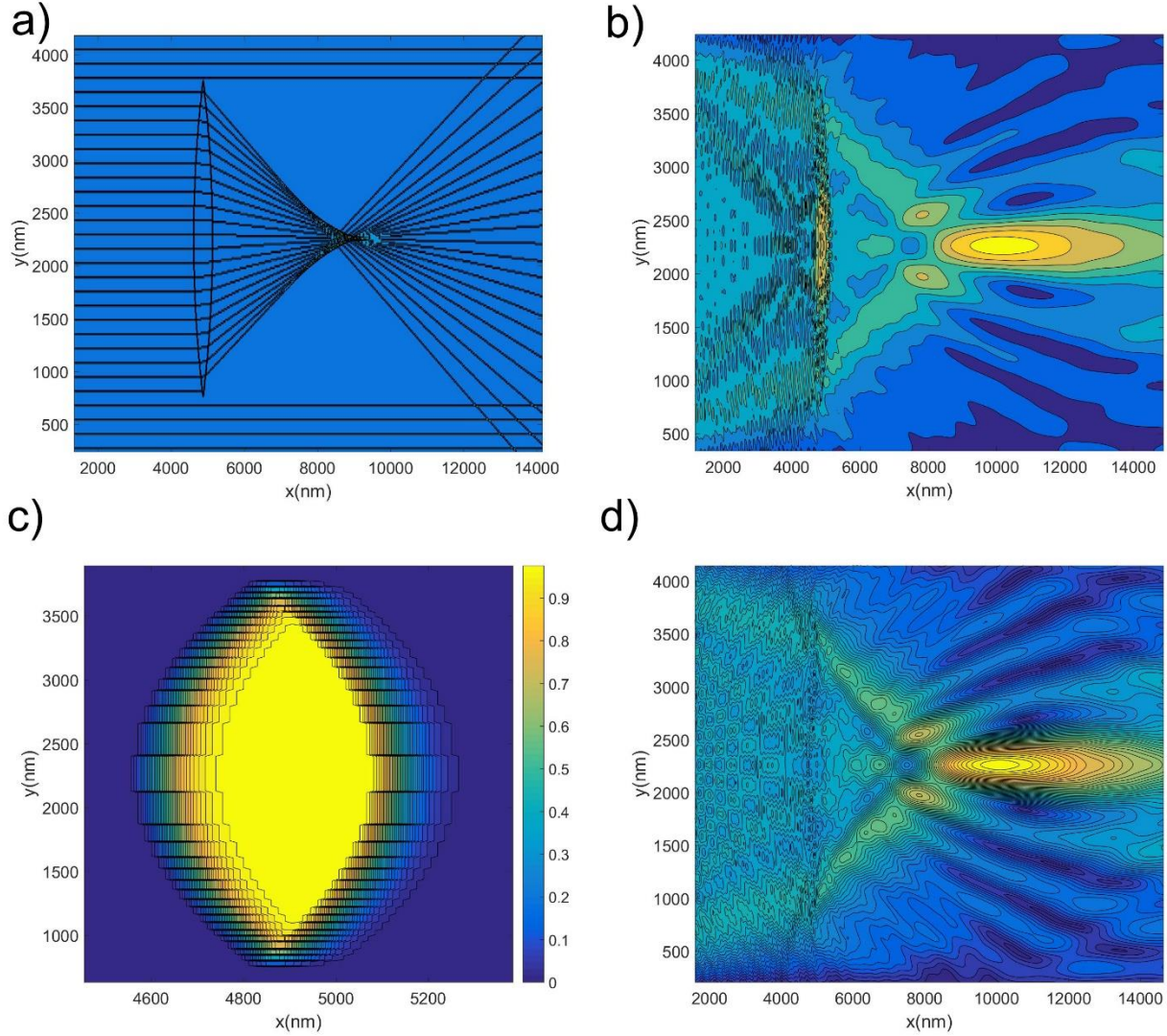


Figure 6. (a) Raytracing model for a compact symmetric lens bounded by the surfaces with curvature radius $R_{1,2} = 4.5$ micrometers, $n_{21} = 1.55$; **(b)** steady state magnetostatic mode amplitudes for an equivalent refractive lens formed by applying $\Delta H = -0.14 \cdot 10^5$ A/m, $\omega = 2.4$ GHz, $H_0 = 2 \cdot 10^5$ A/m; **(c)** normalized equivalent magnetic field profile with Gaussian blur applied and created using a recorded pattern, peak amplitude $\Delta H = -0.14 \cdot 10^5$ A/m, **(d)** steady state magnetostatic mode amplitudes for the magnetic field depicted in (c), $\omega = 2.4$ GHz.

Practical question arises how one can produce such spatially distributed field. It is possible to provide an external magnetic element with an exactly matching shape or to use a specially curved wire, but it is arguably simpler to accomplish the task via a magnetization pattern recorded onto a hard magnetic layer^{10,11,12,13}. Suppose such layer is placed 15nm above the YIG layer, and consists of granular FeCo film with $\mu_0 M_s = 1.6$ T, average grain center to center distance of 7nm with 10% standard variation. Finding the magnetization pattern which corresponds to the desired field profile in the soft media is straightforward since in the Fourier space $\mathbf{M}(\mathbf{k}) = \mathbf{H}(\mathbf{k})/\mathbf{A}(\mathbf{k})$ where $\mathbf{A}(\mathbf{k})$ is a demagnetization tensor

for the given separation between the soft and hard magnetic layers, $\mathbf{H}(\mathbf{k})$ and $\mathbf{M}(\mathbf{k})$ are magnetic field in the soft media and magnetization in the hard layer respectively. Obtained $\mathbf{M}(\mathbf{x}) = \mathcal{F}(\mathbf{M}(\mathbf{k}))$ can then be recreated as best as possible using a simulation of magnetic recording technology, for which we assume a fixed minimal resolution of 12.5 by 50nm, well below the best experimentally demonstrated values. We utilize Heat Assisted Magnetic Recording process¹⁶, in which the hard media is first heated above the Curie temperature and then its magnetization is set via writer's magnetic field. It allows for the saturation of the recorded pattern to be controlled at will and varied smoothly.

However, producing infinitely sharp gradient of the magnetic field requires infinitely large magnetization, making "perfect" lenses (Fig. 5, Fig.6.a) impractical. One of the solutions is to apply a Gaussian blur filter to the desired field distribution (Fig.6.c), so that the resulting magnetic field distribution can then be reproduced via recorded pattern with less than 1% peak error, guaranteeing similar performance (Fig. 6.d) compared to a "perfect" lens modeled with either raytracing (Fig.6.a) or micromagnetics (Fig.6.b). Greatest difference is that "blurred" field profile (Fig. 6.b) produces considerable less reflections. This is also true for optical systems, but in optics using smoothly varied refractive index is difficult.

Both the proposed formulation (Eqs.2-9) and the methodology based on manipulating magnetic refractive index by varying the bias field – are simple in appearance. The consequences though are of considerable importance, allowing for the straightforward adoption of optics based methods such as raytracing as well as individual devices: lenses, reflectors, waveguides and so on. There are but a few restrictions, associated with the fundamental physical differences: magnetostatic waves are predominantly studied as a two dimensional phenomenon and in most cases plasmonic effects can be neglected. Important advantage of working with magnetics is that instead of relying on metamaterials, complex lithography or generally low amplitude magneto-optical or electro-optical phenomena, changing the refractive index by a factor of two or even making it imaginary can be accomplished by simply changing the value of the applied magnetic field, which we can control with a sub-50nm resolution. In addition, one can harness such benefits as operating with wavelengths in sub-100nm range with power consumption orders of magnitude below that of a similar optical device.

References:

1. Chumak, A., Serga A., Hillebrands B., *Magnonic crystals for data processing*, J. Phys. D: Appl. Phys. **50**, 244001-244017 (2017).
2. Puzkarski, H., & Krawczyk, M. *Magnonic Crystals — the Magnetic Counterpart of Photonic Crystals* Solid State Phen. **94**, 125–34 (2003).
3. Demidov V., Demokritov S., Rott K., Krzysteczko P. & Reiss G., *Mode interference and periodic self-focusing of spin waves in permalloy microstripes*, Phys. Rev. B **77**, 064406-064411 (2008).
4. Vlaminck, V., Loayza, N., Castel, V., Stoeffler, D., Bailleul, B. et al., *Near Field diffraction of spin waves*. Colloque Louis Néel XIX (2019).

5. Gräfe J. et al, *Direct observation of spin-wave focusing by a Fresnel lens*, Phys. Rev. B **102**, 024420-024424 (2020).
 6. Toedt, J.N., Mundkowsky, M., Heitmann, D. et al., *Design and construction of a spin-wave lens*, Sci. Rep. **6**, 33169-33173 (2016).
 7. Perez, N. & Lopez-Diaz, L., *Magnetic field induced spin wave energy focusing*, Phys. Rev. B **92**, 014408-014410 (2015).
 8. Whitehead, N., Horsley, S., Philbin, T., Kruglyak, V. *A Luneburg lens for spin waves* Appl. Phys. Lett. **19** 212404-212409 (2018).
 9. Stancil, D., Prabhakar, A., *Spin Waves: Theory and Applications*, Springer (2009).
 10. Papp, Á., Porod, W. & Csaba, G. *Nanoscale neural network using non-linear spin-wave interference*. Nat. Commun. **12**, 6422-6427 (2021)
 11. Rivkin, K. *Magnetic processing unit*, US Patent WO2021016257A1 (2019).
 12. Rivkin, K. & Montemorra, M. *Spin wave computing using pre-recorded magnetization patterns* J. Appl. Phys. **132**, 153902-153911 (2022).
 13. Rivkin, K. *Probabilistic spin wave computing with quasistatic magnetic inputs* J. Appl. Phys. **133**, 213901-213911 (2023).
 14. Klingler, S. et al, *Measurements of the exchange stiffness of YIG films using broadband ferromagnetic resonance techniques*, J. of Phys. D: Appl. Phys. **48**, 015001-015007 (2015).
 15. Rivkin, K., *Calculating dynamic response of magnetic nanostructures in the discrete dipole approximation*, Ph.D. Thesis, Northwestern University (2006).
 16. Granz, S., Rea, C., Ju, G., Czoschke, P., and Hernandez, S., *Heat Assisted Magnetic Recording Areal Density Dependence on Writer Current for Conventional and Shingled Magnetic Recording*, Mag. Rec. Conf. (TMRC), 1-2 (2023).
 17. Born, M., Wolf, E., *Principles of Optics*, Cambridge University Press (1999).
-
-